INTERNATIONAL JOURNAL FOR NUMERICAL METHODS IN FLUIDS
Int. J. Numer. Meth. Fluids 2007; **54**:379–392
Published online 12 December 2006 in Wiley InterScience (www.interscience.wiley.com). DOI: 10.1002/fld.1402

A control volume finite-element method for numerical simulating incompressible fluid flows without pressure correction

Ahmed Omri*, †, Imene Hajri and Sassi Ben Nasrallah

Laboratoire d'Etude des Systèmes Thermiques et Energétiques, Ecole Nationale d'Ingénieur de Monastir, Tunisie, Avenue Ibn Eljazzar, Monastir 5019, Tunisia

SUMMARY

This paper presents a numerical model to study the laminar flows induced in confined spaces by natural convection. A control volume finite-element method (CVFEM) with equal-order meshing is employed to discretize the governing equations in the pressure–velocity formulation. In the proposed model, unknown variables are calculated in the same grid system using different specific interpolation functions without pressure correction. To manage memory storage requirements, a data storage format is developed for generated sparse banded matrices. The performance of various Krylov techniques, including Bi-CGSTAB (Bi-Conjugate Gradient STABilized) with an incomplete LU (ILU) factorization preconditioner is verified by applying it to three well-known test problems. The results are compared to those of independent numerical or theoretical solutions in literature. The iterative computer procedure is improved by using a coupled strategy, which consists of solving simultaneously the momentum and the continuity equation transformed in a pressure equation. Results show that the strategy provides useful benefits with respect to both reduction of storage requirements and central processing unit runtime. Copyright © 2006 John Wiley & Sons, Ltd.

Received 12 July 2006; Revised 5 October 2006; Accepted 15 October 2006

KEY WORDS: equal order; not equal order; coupled strategy; not coupled strategy

1. INTRODUCTION

To benefit from the intrinsic characteristics of the finite-element methods (FEMs) and the control volume methods (CVM) to handle mechanical fluid problems within complex-shaped domains, Baliga and Patankar were the first to propose the concept of control volume finite-element method (CVFEM) [1]. This hybrid method offers the possibility of combining the flexibility of FEM with the easy physical interpretation of CVM. However, the applicability of aforementioned CVFEMs to practical flow problems suffers from intrinsic limitations. More reviews suspect the inexistence

*Correspondence to: Ahmed Omri, Laboratoire d'Etude des Systèmes Thermiques et Energétiques, Ecole Nationale d'Ingénieur de Monastir, Tunisie, Avenue Ibn Eljazzar, Monastir 5019, Tunisia.
†E-mail: ahmed.omri@ipeim.rnu.tn

of pressure equation in incompressible fluid flows to be the cause of many convergence difficulties or spurious oscillations such as the pressure 'checkerboard' problem described in [2, 3]. However, algorithms based on CVFEM for simulating Navies–Stokes equations in arbitrary complex geometries continue to be under intense development and the method remains popular in the numerical modelling. Therefore, modifications and extensions to the original method have been published [4–7].

To overcome difficulties of the velocity–pressure coupling, studies research the adequate meshing and the resourceful interpolation functions for each variable. Baliga [8] first introduced the two shifted meshes type computing the pressure at much fewer grid points than the velocity. This involves the pressure and the velocity on two different sets of elements, called, respectively, macro- and micro-elements. This has made the method quite complex. Additionally, the use of separate computational grids and different families of control volumes for momentum and continuity equations do not guarantee a strict satisfaction of conservation principles over the same control volume for all transported variables. Finally, since the shifted meshes method uses a much coarser grid for pressure, it may not be very accurate for problems with steep pressure gradients. Prackash and Patankar [6], proposed an equal-order procedure using the same control volume for all variables with specific interpolation functions. Sabbas and Baliga [7] asserted that the linear interpolation is sufficient in the treatment of the diffusive case at a time an exponential interpolation is retained for the convective case. Abbassi *et al.* [9] reported that the linear interpolation is more stable than the exponential interpolation.

Moreover, in recent years, claims have emerged for pressure-correction-based schemes. Since then, SIMPLE algorithm and its variants SIMPLER, SIMPLEC, SIMPLESS and SIMPLESSEC have been established [10–12]. Belblidia *et al.* [13] reported that schemes, applied to pressure-driven flows, encounter severe numerical discretization error. This arises in the form of large spatial oscillations across the field and through proper specification of auxiliary (velocity) variables.

The main contribution of this paper is the use of the CVFEM for solving the Navier–Stokes equations in the velocity–pressure formulation without pressure correction using an equal-order (EO) meshing and a not equal-order (NEO) meshing. The EO considers only one control volume where all dependant variables are co-located but the NEO meshing uses two separate grids for the pressure and the momentum.

In the present work, characteristic pressure and velocity interpolations lead to a pressure equation *via* the mass conservation equation. However, the resolution of this equation requires pressure boundary conditions, which are not always available. On the other hand, it is known in fluid mechanics that the knowledge of pressure gradients is more instructive than pressure values. So, the incompressibility condition, when it is verified, is assumed to evade this shortage. In order to assess the capability of the proposed model, the SIMPLER algorithm is used to carry out further results. That allows thorough analyses.

The governing partial differential equations (PDEs) are transformed in nodal algebraic equations *via* integrating over each control volume by use of appropriate interpolation functions. Two strategies are adopted to resolve these equations, called not coupled strategy (NCS) and coupled strategy (CS). In NCS, algebraic equations are resolved separately and, in the CS, the pressure equation and the momentum equations are resolved simultaneously. However, the second strategy leads to sparse and large matrices. Then, the storage technique Yale Sparse Matrix Package [14] is applied.

For solving nodal equations system, conjugate gradient stabilized (CG-Stab) combined with preconditioning symmetric successive over-relaxation (SSOR) is used [15, 16]. The purpose of

DOI: 10.1002/fld

this work is to show that the CVFEMs using the proposed pressure equation with CS and unique meshing are robust for solving the Navier–Stokes.

2. MATHEMATICAL FORMULATION

2.1. Governing equations

The flow is assumed steady and laminar and the fluid properties are assumed constant. The buoyancy effect is considered *via* the Boussinesq approximation. In addition, the pressure work and the dissipation terms are neglected. For any Φ property, which can be diffused and transported by the overall or gross fluid motion, the combined convection and diffusion flux is represented by a vector $\mathbf{j}_\Phi$, generally given in its dimensionless form by:

$$\mathbf{j}_\Phi = \chi \mathbf{v}\Phi - R_\Phi \nabla \Phi \tag{1}$$

χ is constant to be equal to zero when this expression is extended to a non-transportable variable; $\mathbf{v}$ and R_Φ are, respectively, the velocity vector and the corresponding diffusive dimensionless coefficient. The local conservative equation form for the steady two-dimensional incompressible flow is

$$\mathrm{div}(\mathbf{j}_\Phi) = S_\Phi \tag{2}$$

S_Φ is the corresponding volumetric source. It is known that differential equations alone do not specify the problem; we need additional information: boundary conditions for all dependant variables and auxiliary equations allowing diffusion fluxes, body forces and sources to be computed. For the momentum conservation, Equation (2) in steady incompressible cases, depending on an eventual volumetric forces contribution $\mathbf{s}$ and the Reynolds number Re, is

$$(\mathbf{v}.\mathrm{grad}).\mathbf{v} - \frac{1}{Re}\Delta \mathbf{v} = -\mathrm{grad}(p) + \mathbf{s} \tag{3}$$

A general integral formulation corresponding to Equations (2) can be obtained by applying the conservation principle to a control volume Ω that is fixed in space:

$$\int_\Omega \mathrm{div}(\mathbf{j}_\Phi)\, \mathrm{d}\Omega = \int_\Omega S_\Phi \, \mathrm{d}\Omega \tag{4}$$

Table I indicates the dimensionless parameters and variables used in this paper. s_x is equal to zero when the volumetric source reduces to Archimedes forces and (x, y) represent, respectively, the horizontal and the vertical axes.

Table I. Coefficients and source terms in solved equations.

Φ	R_Φ	S_Φ	χ
Mass	0	0	0
Horizontal velocity: u	$1/Re$	$-\frac{\partial p}{\partial x}$	1
Vertical velocity: v	$1/Re$	$-\frac{\partial p}{\partial y} + G_\mathrm{r} T$	1
Temperature: T	$1/Re\,Pr$	0	1

DOI: 10.1002/fld

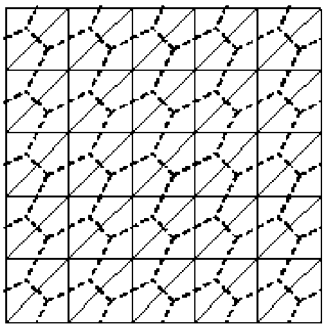

Figure 1. Calculation domain and control volume construction.

2.2. Presentation of the CVFEM

2.2.1. Discretization of the domain (finite elements–control volume). The domain of interest is first divided into three nodes triangular elements, which satisfy the following requirement: do not overlap and, together, fill exactly and completely the calculation domain. The vertices, called nodes, of these triangular elements are the storage locations for dependant variables. Around each node N, a polygonal control volume is constructed by joining the centroid with the middle of each correspondent element side. Figure 1 shows mesh points for pressure and velocity locations.

2.2.2. Interpolation functions. Using appropriate interpolation functions, integral (4) provides an algebraic system in terms of the variable's values at the nodal locations. In this respect, Baliga and Patankar [1] developed an approach inspired by the unidirectional convection–diffusion problems. When a laminar flow is developed in one direction with a uniform velocity u parallel to the x-axis, Equation (3) admits the following analytical solution: $\Phi(x) = \Phi_0 \exp((u/R_\Phi)x)$.

This solution can be extended to any flow without source term in an elementary space where the flow is assumed unidirectional. Hence, one can define an approximate solution, which must favour the convective transport in the main flow direction and take account of the diffusion in transversal direction in each finite element as

$$\Phi(X, Y) = A^\Phi \exp\left(\frac{V}{R_\Phi} X\right) + B^\Phi Y + C^\Phi \tag{5}$$

X and Y represent a local Cartesian coordinate system of whom the origin is located at the centroid G of the element. The first axis aligns with the average velocity direction and the second with the direct perpendicular axis. Obviously, when the diffusion is dominant, the variable Φ is bilinear. All coefficients (A^Φ, B^Φ, C^Φ) must be evaluated by requiring the correspondent interpolation function to assure the nodal values of the considered variable. Each coefficient can be expressed in terms of the nodal coordinates and the nodal values of the corresponding variable.

This function, used by Omri and Nasrallah [17], Alimi *et al.* [18] and Omri *et al.* [19] is of the flow-oriented upwind type but difficulties signalized in [7] are not remarked.

The pressure, which is not an extensive variable, can be assumed bilinear in each finite element:

$$p = A^p \cdot x + B^p \cdot y + C^p \tag{6}$$

DOI: 10.1002/fld

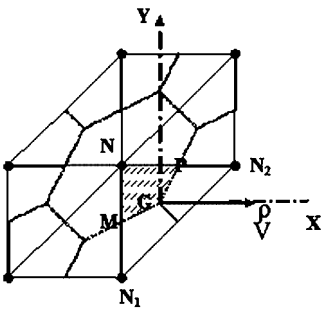

Figure 2. Sub-control volumes: local coordinates system.

When Equation (6) is required to assure the nodal values of the pressure, all coefficients (A^{p}, B^{p}, C^{p}) will be evaluated and expressed in terms of the nodal coordinates and the nodal pressure values.

2.2.3. Algebraic equations.

2.2.3.1. General form for dependant variables. Using Equations (5) and (6), integral (4) can be calculated over the control volume rounding each node N. As shown in Figure 2, each node is the summit of a number E of finite elements, as $\mathrm{NN_1N_2}$, which contribute to the control volume by sub-volumes as $MG_i P$.

Using the theorem of Green–Ostrogradsky and the Simpson role, this integrating must be over each sub-volume and transforms in a nodal equation:

$$\sum_{i=1}^{i=K} (a_i^{\Phi} \Phi_i) = B_{\mathrm{N}}^{\Phi} \tag{7}$$

In this equation, the last term includes the term source contributions but the pressure must appear only when Φ represents the velocity components u and v.

2.2.3.2. Algebraic pressure equation. In integral form, over the control volume corresponding to node N, the mass conservation is expressed, for incompressible fluid flow as

$$\int_{\Omega} \mathrm{div}(\mathbf{v})\, \mathrm{d}\Omega = 0 \tag{8}$$

Using a bilinear interpolation for each velocity component, this integral transforms in a nodal algebraic equation as

$$\sum_{i=1}^{i=K} (a_i^u u_i) + \sum_{i=1}^{i=K} (a_i^v v_i) = 0 \tag{9}$$

This equation transforms in a pressure equation when u and v are extracted from corresponding Equations (7). At node N, these components can be expressed by relative pseudo-velocities

DOI: 10.1002/fld

$\hat{u}_N$ and $\hat{v}_N$ as

$$u_N = \hat{u}_N + \sum_{i=1}^{i=K} (a_i'^v p_i) \tag{10a}$$

$$v_N = \hat{v}_N + \sum_{i=1}^{i=K} (b_i'^v p_i) \tag{10b}$$

Using Equations (6), (9), (10), the pressure equation appears as

$$\sum_{i=1}^{i=K} (a_i^p p_i) = S_N^p \tag{11}$$

2.3. Solution method

2.3.1. Strategies. At each node, an algebraic equation is established for each variable. On that, when the domain discretization leads to n control volumes (CVs), the algabraic system includes n blocks of five equations: two for pseudo-velocities, two for velocity components and one for the pressure. These equations are intricately coupled by the dynamic system variables and great care must be taken in order to achieve a convergent simulation result. There are two possibilities for solving this deposit. First, the NCS which solves separately and successively the set of Equations (7), (11) for the velocity components and the pressure. Second, the CS that sets these equations in a global matricide form

$$AX = B \tag{12}$$

Each component of the vector X corresponds to one amongst five desired variables. A, viewed entierly, is $n \times n$ block matrix having internal sub-blocks of size 5×5. The efficient resolution of this type of system can be expensive and then it is imperative to take into account the inherent blocks nature by the use of a good iterative technique. To manage memory storage requirements, a data storage based on Yale Sparse Matrix Package [15, 16] is used.

2.3.2. Sparse matrix solver. Given the linear sparse matrix system for each inner linearization step and some of initial solution $X^{(0)}$, the numerical resolution consists of annulling the vector $AX - B$ which can be considered as the gradient of the quadratic function: $f(X) = X^T AX - X^T B$. This can be achieved by the conjugate gradient schemes. For all of the tests performed in this work, we select the bi-conjugate gradient stabilized (Bi-CGSTAB) which is the most popular generation of the later CG Method. This provides a smooth convergence behaviour by employing steepest descent steps at each iteration [15, 16].

2.3.3. Preconditioner. In an attempt to reduce the overall computation time, system (12) is modified by an adequate preconditionning: $(PA)X = PB$. The well-known incomplete factorization level zero, ILU(0), has been selected in this study. For this preconditionning matrix, the structure of the decomposed matrix ILU is consistent with the structure of the original A matrix and no extra fill is added [20].

DOI: 10.1002/fld

2.3.4. Computational procedure. The resolution is illustrated by the following sequences:

Step 1: Guess initial values for each unknown variable and apply boundary conditions for velocity components and any other dependent variable Φ.

Step 2: Calculate coefficients for the pseudo-velocity, the velocity and the pressure equations.

Step 3: Solve the algebraic system (12).

Step 4: Calculate all coefficients for each other dependant variable equation.

Step 5: Solve for other dependent variables.

Step 6: Check for convergence: if the criteria are not satisfied then return to step 2.

The discrepancies between the grid dimension in terms of select flow and thermal quantities were compared considering also the central processing unit (CPU) times required on a Pentium IV, 1.6 MHz processor. A grid density of 51×51 was chosen for the calculation of all cases. Solutions were assumed to converge when the following convergence criteria were satisfied for every variable at every node in the solution domain:

$$\left| \frac{\phi^k - \phi^{k-1}}{\phi^{k-1}} \right| < \varepsilon$$

ε is fixed below 10^{-3}, k and $k-1$ refer, respectively, to a present iteration and the precedent iteration; ϕ represents u, v, p and variables Φ.

To prevent eventual divergence or oscillatory convergence experimented when the change in the solution field, from iteration to the next, the computing is controlled by the underrelaxation techniques described by Van Doormal and Raithby [10]. In order to ensure the mass conservation at each iteration end, this is also done for the pressure equation.

3. APPLICATION TO TEST PROBLEMS

The code, elaborated by using the CVFEM and the numerical schemes presented in the second section, was validated by comparing against well-known analytical or numerical results available in the literature relative to laminar flow studies. Therefore, in this section, the validation and the analysis concern three test problems, which are *the flow between concentric rotating cylinders*, *the driven cavity* and *the natural convection in a square cavity*.

Before the main course of the computations, a numerical experiment was carried out for grid-independence test. Results on $11 * 11$, $21 * 21$, $31 * 31$, $35 * 35$, $41 * 41$ and $45 * 45$ grids were examined. The solutions on $35 * 35$ are very close than those of $41 * 41$ but the solutions on $41 * 41$ and on $45 * 45$ agree well. To reduce the computational efforts, therefore, the $41 * 41$ grid was chosen for the calculations through the entire study. As in [21], the grid system is a uniform one.

3.1. Flow between concentric rotating cylinders

Consider the isothermal flow of an incompressible fluid between two concentric cylinders.

The inner cylinder is at rest, while the outer cylinder is in a uniform rotation. The exact solution for this problem can be found in Reference [22]. In the x–y Cartesian coordinates, the problem is fully two dimensional with velocity component u and v along the x and y coordinates, respectively.

DOI: 10.1002/fld

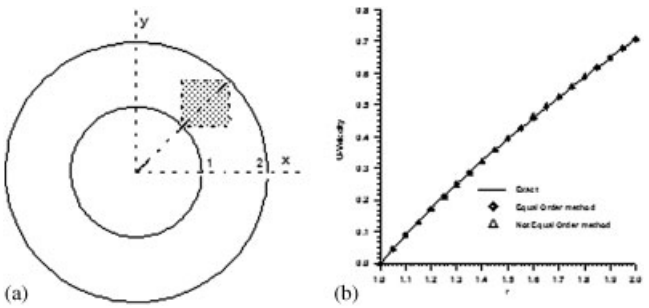

Figure 3. Concentric rotating cylinders: (a) domain of interest; and (b) the profile of the horizontal velocity component along the diagonal.

The analytical dimensionless solution is

$$u = \frac{2}{3} y \left(1 - \frac{1}{r^2}\right), \quad v = -\frac{2}{3} x \left(1 - \frac{1}{r^2}\right) \quad \text{and} \quad p = y \left(1 - \frac{1}{r^2}\right)$$

Dimensionless variables are defined by reference to r_1 for distances, $r_1\omega$ for velocities and $\rho r_1^2 \omega^2$ for pressure. Figure 3(a) indicates the calculation domain in the annular space. For the boundary conditions, both u and v were prescribed using the exact solution. Figure 3(b) shows the profile of the horizontal velocity component along the main diagonal. One can see that the computed results are in a good agreement with the exact solution.

In order to compare different strategies, we define an infinity error for each iteration as

$$\chi = \mathrm{Log} \left| \frac{\phi^{k+1} - \phi^k}{\phi^{k+1}} \right|$$

The convergence rate is depicted in Figure 4 representing the CPU time used by the EO and NEO methods for a Reynolds number equal to 200. One can remark that the NEO is faster than the EO (Figure 4(a)). This result is predictable seeing that computing the pressure over coarse grid needs less calculation. However, as it can be pointed out from Figure 4(a) and (b), the SIMPLER algorithm enhances the convergence quickness both for EO and NEO methods.

Elsewhere, Figure 4(c) shows that the NEO method together with the CS requires 50% less CPU time than NCS.

For a close comparison in term of precision, we define relative error as

$$\%\mathrm{error} = \left| \frac{\phi_{\mathrm{exact}} - \phi_{\mathrm{computed}}}{\phi_{\mathrm{exact}}} \right|$$

Tables II and III give the velocity components values at the midpoint of the computational domain. Obviously, the EO and NEO methods are competitive but regarding the precision over all nodes, the first method gives lower errors. Table IV relates the swerving of the present results on the exact solution.

DOI: 10.1002/fld

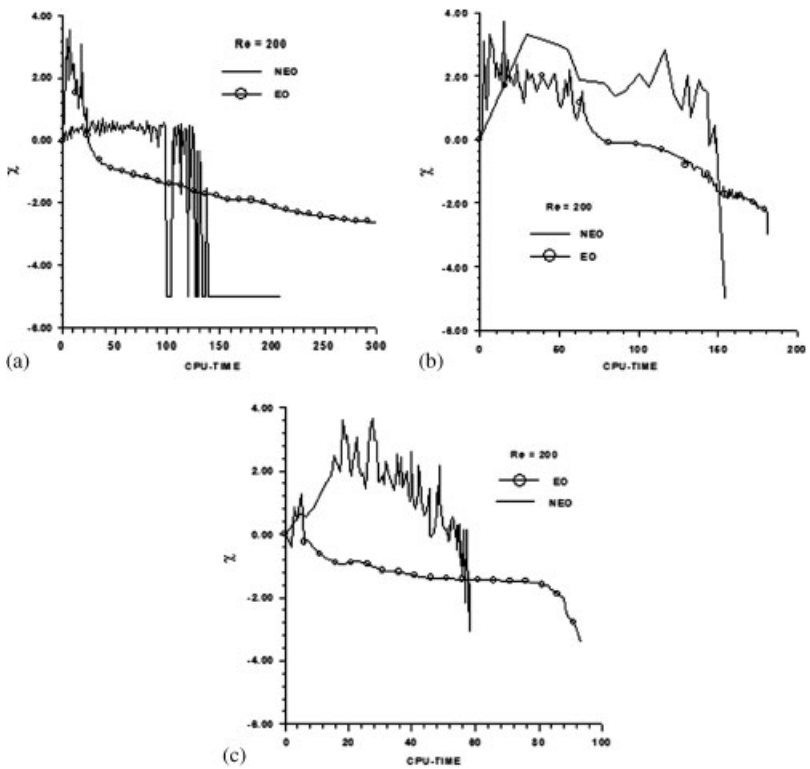

Figure 4. Concentric rotating cylinders: infinity error norm on pressure for $Re = 200$.

Table II. Relative error at the centre of the domain equal-order method.

	Solutions	Horizontal velocity	Vertical velocity
$Re = 100$	Analytical	0.3928	−0.3928
	Numerical	0.3925	−0.3924
	Error (%)	0.08	0.1
$Re = 400$	Analytical	0.3928	−0.3928
	Numerical	0.3924	−0.3924
	Error (%)	0.1	0.1

3.2. The driven cavity problem

The second test problem concerns a steady laminar flow of an incompressible Newtonian fluid in a square enclosure. As illustrated in Figure 5(a), a sliding lid generates the fluid motion at the top boundary. Three sides of the cavity are at rest while the fourth, the top wall, moves tangentially with velocity u_0. The depth of the enclosure perpendicular to the diagram is assumed long and

DOI: 10.1002/fld

Table III. Relative error at the centre of the domain not equal-order method.

Re	Solutions	Horizontal velocity	Vertical velocity
100	Analytical	0.3928	−0.3928
	Numerical	0.3932	−0.4121
	Error (%)	0.1	5
400	Analytical	0.3928	−0.3928
	Numerical	0.3952	−0.3943
	Error (%)	0.6	0.4

Table IV. Average relative error over the domain equal and not equal-order methods.

	Equal-order method		Not equal-order method	
Re	Horizontal velocity (%)	Vertical velocity (%)	Horizontal velocity (%)	Vertical velocity (%)
100	0.101	0.090	0.217	0.252
400	0.124	0.113	0.621	0.531

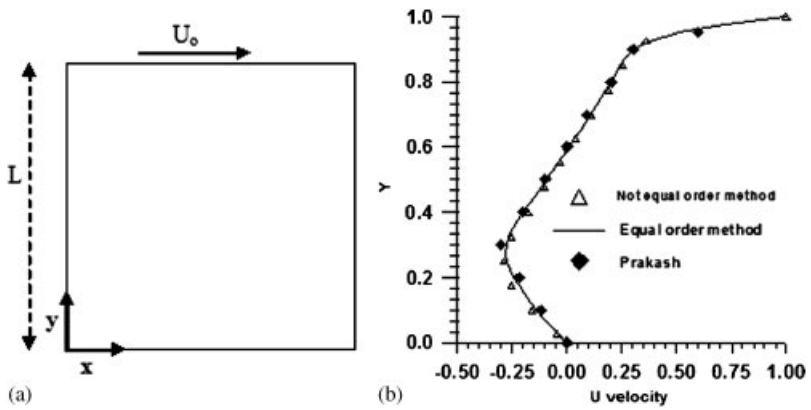

Figure 5. (a) Driven cavity; and (b) velocity profile at the midplane.

the problem can be considered two dimensional. The velocity is equal to zero on the bottom and on each vertical wall. The dimensionless velocity components on the top wall are $u = 1$, $v = 0$.

Figure 5(b) presents the profile of the horizontal velocity at the vertical centreline for $Re = 400$. As it can be seen, the performance of the proposed EO and NEO methods is illustrated. However, the result carried out by EO method is more close to that of Reference [5]. Table V shows the velocity components values at the domain centre. The relative error obtained by the EO method is less than the error obtained by the NEO method.

DOI: 10.1002/fld

Table V. Values of the velocity components at the centre.

	$Re = 100$		$Re = 400$	
Methods	u	v	u	v
Equal order	−0.199	0.05	−0.104	0.056
Not equal order	−0.186	0.045	−0.085	0.041
Ghia and Ghia [23]	−0.20581	0.05454	−0.1147	0.05186

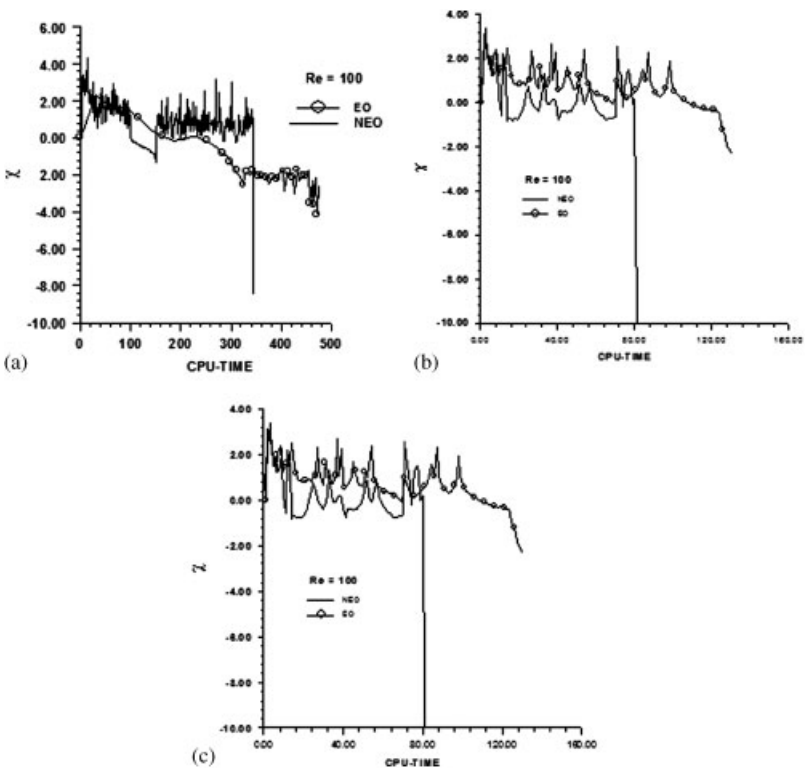

Figure 6. Driven cavity-infinity error norm on pressure for $Re = 100$: (a) not coupled strategy; (b) not coupled strategy with SIMPLER; and (c) coupled strategy.

Figure 6 summarizes the comparison of the CPU time for the driven cavity problem using EO and NEO. The convergence with CS is faster than the NCS.

3.3. Natural convection in a square cavity

The physical system of the natural convection in a square cavity is schematically shown in Figure 7(a). The hot and cold vertical walls are both isothermal, having temperature $T_h = 1$ and $T_c = 0$, respectively. The top and the bottom are assumed adiabatic. The fluid is assumed incompressible and the flow is governed by Boussinesq hypothesis.

DOI: 10.1002/fld

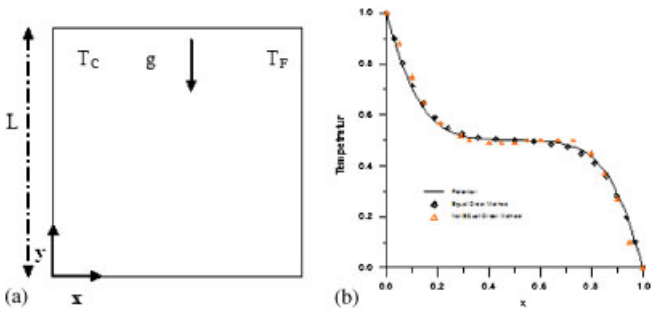

Figure 7. (a) Natural convection in the square cavity; and (b) temperature profile at the midplane.

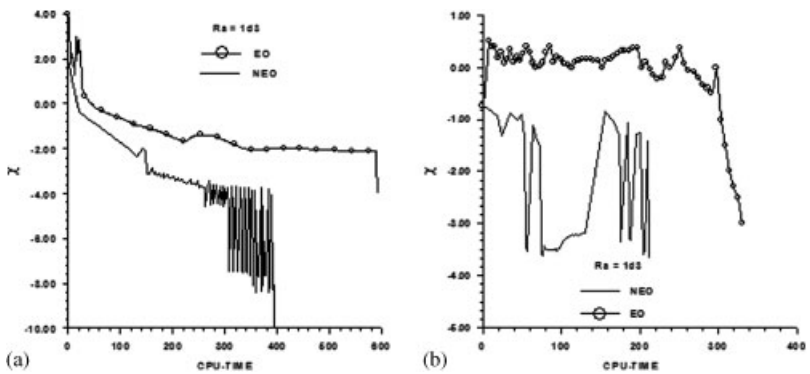

Figure 8. Natural convection in a square cavity: infinity error norm on pressure for $Ra = 1000$: (a) not coupled strategy; and (b) coupled strategy.

Figure 7(b) shows the temperature profile along the horizontal midplane for $Ra = 10^4$ using the EO method and NEO method. The result is in concordance with the solution published by Patankar [6]. Obviously, the EO method provides result more close to the reference.

Figure 8 shows the convergence rate expressed in terms of CPU. The CS reduces noticeably the convergence time for both methods.

4. CONCLUSION

A numerical model, based on the control volume finite-element methods was proposed to resolve Navier–Stokes equations in the primary formulation (velocity–pressure). Two schemes, equal order and not equal order, were used to discretize the domain of interest and two strategies, coupled strategy and not coupled strategy, were used to resolve the algebraic system. Three problems in the domain of fluid flow and heat transfer are investigated. A comparison about precision and convergence rate has been done.

DOI: 10.1002/fld

Results indicate that the use of a coarser grid for pressure improves the convergence rate but reduces the precision of the solution. The equal order is more accurate than the not equal order but the second is more rapid. When the algebraic system relative to the nodal momentum and the pressure is set as a unique equation, the resolution requires less time than the separate resolution. Then, algorithms using the not equal-order method with the coupled strategy are faster than the equal order with the not coupled strategy.

NOMENCLATURE

g	gravitational acceleration
p	dimensionless pressure
Pr	Prandtl number
Ra	Raleigh number
Re	Reynolds number
T	non-dimensional temperature
u, v	Cartesian velocity components
V	average velocity magnitude
x, y	coordinates
X, Y	local coordinates

Subscripts

e	element
nb	neighbours of point P
P	pertaining to typical grid point

REFERENCES

1. Baliga BR, Patankar SV. A control volume finite-element method for two-dimensional fluid flow and heat transfer. *Numerical Heat Transfer* 1980; **6**:245–262.
2. Patankar SV. *Numerical Heat Transfer and Fluid*. Hemisphere: Washington, DC, 1980.
3. Baliga BR, Patankar SV. A new finite element formulation for convection–diffusion problems. *Numerical Heat Transfer* 1983; **3**:245–262.
4. Baliga BR, Pham TT, Patankar SV. Solution of some two-dimensional incompressible fluid flow and heat transfer problems using a control volume finite element method. *Numerical Heat Transfer* 1983; **6**:263–282.
5. Prackash C. An improved control volume finite-element method for heat and mass transfer, and for fluid flow using equal order velocity pressure interpolation. *Numerical Heat Transfer* 1986; **9**:253–276.
6. Prackash C, Patankar SV. A control volume based finite element methods for solving the Navies–Stokes equations using equal order velocity pressure interpolation. *Numerical Heat Transfer* 1985; **8**:259–280.
7. Sabbas HJ, Baliga BR. Co-located equal order control-volume finite element method for multidimensional, incompressible, fluid flow. Part I: Formulation. *Numerical Heat Transfer*, *Part B* 1994; **26**:381–407.
8. Baliga BR. A control-volume based finite element method for convective heat and mass transfer. *Ph.D. Thesis*, University of Minnesota, Minneapolis, U.S.A., 1978.
9. Abbassi H, Turki S, Ben Nasrallah S. Interpolation function in control volume finite element method. *Computational Mechanics* 2003; **30**:303–309.
10. Van Doormal JP, Raithby G. Enhancement of the SIMPLE method for predicting incompressible fluid flow problems. *Numerical Heat Transfer* 1984; **7**:147–163.
11. Shaw GJ, Sivaloganathan S. The SIMPLE pressure-correction method as a non-linear smoother. *Notes on Numerical Fluid Mechanics* 1988; **29**:574–581.

DOI: 10.1002/fld

12. Gjesdal T, Lossius MEH. Comparison of pressure correction smoothers for multigrid solution of incompressible flow. In *Multigrid Methods V*, Hackbusch W, Wittum G (eds). Springer: Berlin, 1995.
13. Belblidia F, Keshtiban IJ, Webster MF. Novel schemes for steady weakly compressible and incompressible flows. *Computer Science Report Series 8*, University of Wales, Swansea, 2003.
14. Duff IS, Erisman AM, Reid JK. *Direct Methods for Sparse Matrices*. Clarendon Press: Oxford, 1986.
15. Zhang SL. A class product-type Krylov-subspace methods for solving nonsymmetric linear systems. *Journal of Computational and Applied Mathematics* 2002; **149**:297–305.
16. Tuff AD, Jennings A. An iterative method for large systems of linear structural equations. *International Journal for Numerical Methods in Engineering* 1973; **7**(2):175–183.
17. Omri A, Nasrallah SB. Control volume finite element numerical simulation of mixed convection in an air-cooled cavity. *Numerical Heat Transfer* 1999; **36**:615–637.
18. El Alimi S, Orfi J, Nasrallah SB. Buoyancy effects on mixed convection heat and mass transfer in a duct with sudden expansions. *Heat and Mass Transfer* 2005; **41**:559–567.
19. Omri A, Orfi J, Nasrallah SB. Natural convection effects in solar stills. *Desalination* 2005; **183**:173–178.
20. Behie GA, Forsyth Jr PA. Incomplete factorization methods for fully implicit simulation of enhanced oil recovery. *SIAM Journal on Scientific Computing* 1984; **5**(3):543–561.
21. Hajri I, Omri A, Ben Nasrallah S. A numerical model for the simulation of double-diffusive natural convection in a triangular cavity using equal order and control volume based on the finite element method. *Desalination* 2007; **206**:579–588.
22. Ramadhiani S, Patankar SV. Solution of the convection–diffusion equation by a finite-element method using quadrilateral elements. *Numerical Heat Transfer* 1985; **8**:595–612.
23. Ghia KN, Ghia U. *Parabolic Systems*: *Finite-Difference Method II*, *Handbook of Numerical Heat Transfer A*. Wiley-Interscience: New York, 1988; 293–346.

DOI: 10.1002/fld